Geomorphology 106 (2009) 242–252

Contents lists available at ScienceDirect

Geomorphology

journal homepage: www.elsevier.com/locate/geomorph

Examining the physical meaning of the bank erosion coefficient used in meander migration modeling

Candice R. Constantine [a,*], Thomas Dunne [a,b], Gregory J. Hanson [c]

[a] Department of Earth Science, University of California, Santa Barbara, CA 93106, USA
[b] Donald Bren School of Environmental Science and Management, University of California, Santa Barbara, CA 93106, USA
[c] USDA-ARS Hydraulic Engineering Unit, 1301 N. Western Road, Stillwater, OK 74075, USA

ARTICLE INFO

Article history:
Received 28 October 2008
Received in revised form 5 November 2008
Accepted 7 November 2008
Available online 14 November 2008

Keywords:
Fluvial geomorphology
Bank erosion
Meandering
Riparian vegetation
Alluvial rivers
Erodibility

ABSTRACT

Widely used models of meander evolution relate migration rate to vertically averaged near-bank velocity through the use of a coefficient of bank erosion (E). In applications to floodplain management problems, E is typically determined through calibration to historical planform changes, and thus its physical meaning remains unclear. This study attempts to clarify the extent to which E depends on measurable physical characteristics of the channel boundary materials using data from the Sacramento River, California, USA. Bend-average values of E were calculated from measured long-term migration rates and computed near-bank velocities. In the field, unvegetated bank material resistance to fluvial shear (k) was measured for four cohesive and noncohesive bank types using a jet-test device. At a small set of bends for which both E and k were obtained, we discovered that variability in k explains much of the variability in E. The form of this relationship suggests that when modeling long-term meander migration of large rivers, E depends largely on bank material properties. This finding opens up the possibility that E may be estimated directly from field data, enabling prediction of meander migration rates for systems where historical data are unavailable or controlling conditions have changed. Another implication is that vegetation plays a limited role in affecting long-term meander migration rates of large rivers like the Sacramento River. These hypotheses require further testing with data sets from other large rivers.

1. Introduction

Physically based meander migration models developed from the theory of Ikeda et al. (1981) and Johannesson and Parker (1989) have been used to investigate the long-term (i.e., decades to thousands of years) evolution of meandering river planform (Stølum, 1998; Sun et al., 2001a,b) and floodplain morphology (Howard, 1992; Sun et al., 1996). Shorter term (i.e., decades to years) river responses to management decisions have also been predicted (Larsen and Greco, 2002; Larsen et al., 2006). In these models, the rate of meander migration (M) is predicted from the equation

$$M = E \cdot u_b' \tag{1}$$

where E is a coefficient of bank erosion and u_b' is the difference between the depth-averaged near-bank velocity and the cross-sectionally averaged velocity (Ikeda et al., 1981). Field studies by Pizzuto and Meckelnburg (1989) provided evidence in support of a linear relationship between M and u_b', which reflects the magnitude of the shear forces acting on the bank. In predictions using Eq. (1), the coefficient E is typically determined through calibration to historical planform changes (e.g., Larsen and Greco, 2002); therefore, the meaning of E and the extent to which it depends on physical characteristics of the channel or the bank material remain unclear. Researchers generally agree that E reflects the geotechnical properties of the bank material (Hasegawa, 1989; Wallick et al., 2006) and the effects of vegetation on near-bank flow and bank strength (Odgaard, 1987; Pizzuto and Meckelnburg, 1989; Micheli and Kirchner, 2002a; Micheli et al., 2004). The coefficient may also vary with other channel characteristics such as bank height and local channel slope (Hasegawa, 1989), local channel width (Larsen, 1995; Wallick et al., 2006), and the availability of sediment for deposition on point bars (Ikeda et al., 1981).

Other models have been developed in which bank migration results from intermittent bank collapse in response to a slope-stability criterion instead of depending on calibration to link flow conditions in the channel to the rate of erosion at the bank (Nagata et al., 2000; Darby et al., 2002). Despite this benefit, mechanistic models of bank erosion face the limitation that they are specific to a particular type of bank material or failure mechanism. For example, the model of Darby et al. (2002) predicted the rate of bank retreat via planar failure. Although planar failures are common at steep river banks (Thorne,

* Corresponding author. Current address: 61 Ninian Road, Flat 2, Roath Park, Cardiff CF23 5EL, UK.
E-mail addresses: candice.constantine@gmail.com (C.R. Constantine), tdunne@bren.ucsb.edu (T. Dunne), greg.hanson@ars.usda.gov (G.J. Hanson).

0169-555X/$ – see front matter © 2008 Elsevier B.V. All rights reserved.
doi:10.1016/j.geomorph.2008.11.002

1982), other types of failures are frequently observed in the field. Failures may be rotational where bank material is cohesive (e.g., Brunsden and Kesel, 1973) or cantilever where banks are stratified (Thorne and Tovey, 1981). The occurrence of failure in these cases is driven by the fluvial removal of sediment at the base of the bank. As a result of this natural variability in river bank type, failure, and sediment removal processes, mechanistic approaches are not as broadly applicable as the linear approach in Eq. (1).

The purpose of this study is to make progress toward developing the capability to estimate E from field measurements of bank material properties. The ability to define E without calibration is particularly useful for understanding the rate-limiting controls on bank migration and for predicting migration of rivers for which historical planform data are unavailable or flow and bank conditions have recently changed. One of the hindrances to doing this in the past was the lack of a quantitative field method to measure directly the erodibility of both cohesive and noncohesive banks. This limitation is addressed here by using a recently developed jet-test apparatus and test procedure (Hanson, 1990; Hanson et al., 2002; Hanson and Cook, 2004). The procedure was designed to measure the erosion resistance of both cohesive and noncohesive banks by subjecting the bank material *in situ* to a realistic fluvial shear rather than use a penetrometer or shear vane or other geotechnical index of resistance to collapse. During the course of the test, a known shear stress is applied to the bank *in situ* through a submerged jet apparatus, and the erosion rate of the bank is measured. The relationship between the applied stress and the erosion rate is used to determine the critical shear stress and an erodibility coefficient k that describes bank material resistance to erosion by fluvial shear.

In this study, the results of jet tests completed on four different bank material types were compared with E values calculated from historical migration rate data and Eq. (1). To examine the influence of other channel conditions on E, values of the coefficient were also compared with data on land cover, proximity to bank-protection structures, local width-to-depth ratio, local slope, local bank height, local average velocity, bed material grain size, and bed material storage change. Results suggest a strong correlation between E and k, which implies that E may be determined directly from field measurements of bank material resistance to fluvial shear. Such an approach would allow for predictions of meander migration that are independent of past patterns of channel shifting. The correlation between E and k also suggests that bank material properties are the predominant control on long-term meander migration rates of the Sacramento River and perhaps other large rivers with vegetation playing a more limited role. This hypothesis requires further testing with more data from other large rivers.

2. Study area

The Sacramento River drains 68,000 km^2 of northern California, USA. Its basin has a Mediterranean climate characterized by cool, wet winters and warm, dry summers. Average annual precipitation ranges from 50 cm/y on the valley floor to 178 cm/y in the surrounding mountains (California Department of Water Resources, 1994). The study area is an 85 km sinuous portion of the lowland river between Hamilton City (RM 196) and Colusa (RM 144) that exhibits active lateral migration (Fig. 1). As a result of lateral shifting, river mile markers no longer correspond with actual streamwise distance; however, river mile designations are used as longitudinal reference points in this study in accordance with published works by the different researchers and agencies working in the watershed. For this reason, locations are referred to in river miles, whereas all calculations are expressed in metric units.

Peak flows in the Sacramento occur in the winter and spring when the basin receives most of its precipitation and snow melt. The natural hydrograph was altered in 1943 with the closure of Shasta Dam, which had the effect of dampening flood peaks and elevating low summer flows (Singer, 2007). The 2 year flood at the upstream end of the study area is ~2550 m^3/s [U.S. Geological Survey (USGS) gauge 11383800]. Discharge declines downstream as overbank flow is routed to Butte Basin across the floodplain and through Moulton and Colusa weirs where the channel and proximal floodplain are lined by levees (Fig. 1). The 2 year flood at Colusa is 1125 m^3/s. Average bankfull width follows discharge, declining from 340 m near Hamilton City to 150 m at Colusa. Channel slope also declines downstream from 0.0005 near Hamilton City to 0.0002 at Colusa. The channel bed throughout the study area is composed of a poorly sorted mixture of gravel and sand. Gravel dominates the mixture upstream, but sand makes up more than 25% of the bed downstream of RM 160.

Natural river banks in the study area are primarily composed of two types of material: relatively erosion-resistant Quaternary terrace material and younger unconsolidated Holocene alluvium. The Quaternary Riverbank and Modesto Formations form two sets of terraces that border the Holocene meander corridor. The Riverbank Formation, which contains numerous partially cemented and cohesive layers (Smith and Verrill, 1998), is more resistant to erosion. Both the Modesto and the Riverbank Formations are in places underlain by cemented Quaternary and Tertiary deposits. Banks composed of Holocene alluvium typically have a lower layer of noncohesive gravel and sand and an upper layer of silt; grain size and sand content of the gravel base vary widely. Variations within the Holocene alluvium include banks that are mainly sand and lack a gravel base and banks that have a high percentage of clay and represent oxbow lake fill.

The average 50 year meander migration rate in the study area is about 4 m/y, but single-bend rates range from 0 m/y where the river abuts terrace material to 10 m/y at unconstrained bends (Constantine, 2006). Although levees are present in the downstream portion of the study area, they are set back from the river and spaced 0.75 to 2.5 km (~1.0 to 3.3 times meander amplitude) apart (Fig. 1), encompassing both the channel and proximal floodplain and allowing channel shifting to occur. Bank-protection structures, primarily rock revetment and concrete rubble, are present in most reaches and cover about 20% of the bankline in the study area (California Department of Water Resources, 1994). Included in this total are most of the locations downstream of RM 175 where the river abuts a levee and where rock and concrete serve as protection against levee degradation. Only freely migrating bends were included in the analyses conducted for this study.

3. Methods

3.1. Measuring migration rates

Rates of lateral migration for individual bends were measured for the period 1978–2004. This time period was chosen because it captured a number of large erosion events and includes the post-1997 time period for which bed material transport and storage changes were modeled (see Constantine, 2006). Digital copies of aerial photographs taken in May 1978 by the U.S. Department of Agriculture (USDA) (scale 1:40,000) were obtained from the California Department of Water Resources (DWR), Northern District. Orthorectification of the photos was completed in ENVI (Research Systems, Inc.) using USGS orthophoto quadrangles as base photos, a digital elevation model (DEM) from the USGS National Elevation Dataset, and the appropriate USDA camera calibration report. The average horizontal accuracy achieved was 3.5 m (root mean square error). Orthorectified 2004 photos (1.9 m root mean square error) were obtained from AirPhotoUSA.

Thalweg centerlines for 1978 and 2004 were digitized and intersected to define polygons that represent areas of floodplain eroded over the 26 year period. Centerlines were drawn through small mid-channel bars and, in multithreaded segments of the river, were drawn around larger bars and islands, tracing the path of the widest (main) channel. Following a method by Micheli (2000), the average migration rate for

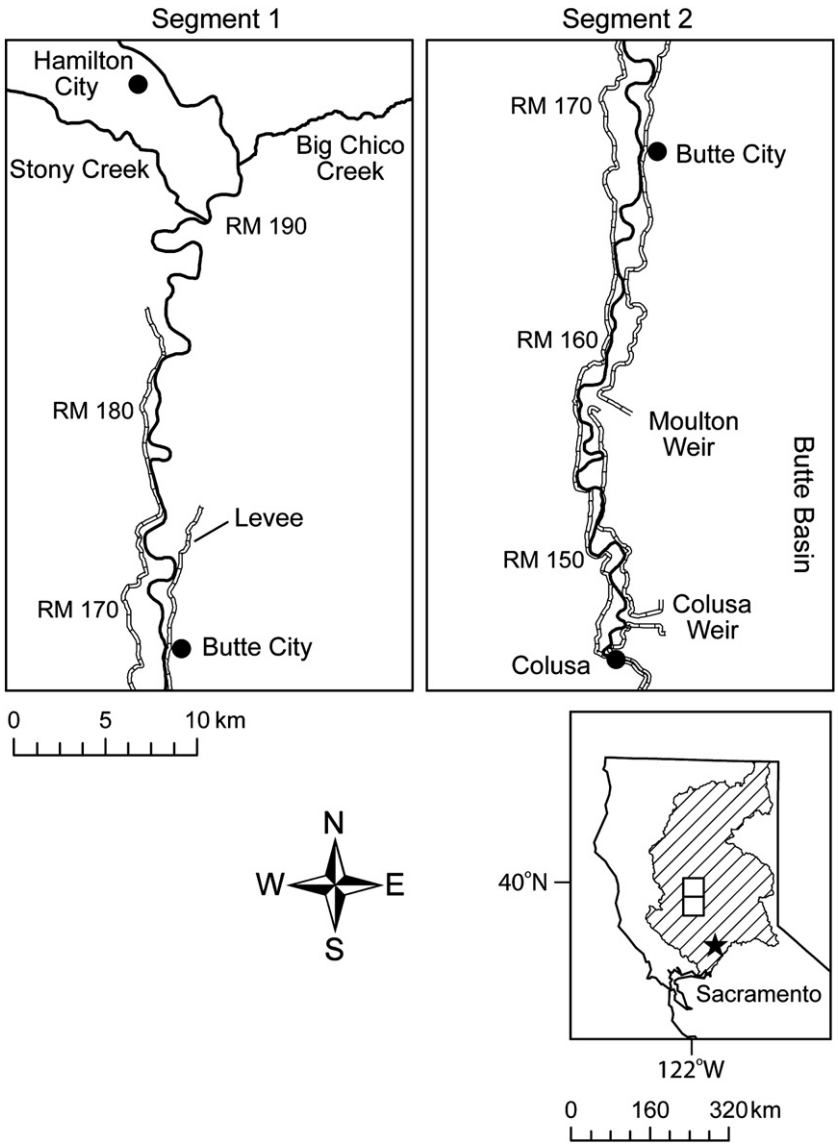

Fig. 1. Sacramento River study area location map. Segments for computing u_b' were determined based on differences in channel width and slope.

each eroded-area polygon was computed by dividing the polygon area by one-half its perimeter and by the number of years elapsed between the centerline dates (Fig. 2). This method provides estimates of minimum average migration rate because the direction of channel shifting may have reversed at least once between 1978 and 2004. Polygons formed where cutoff occurred were excluded from the analysis.

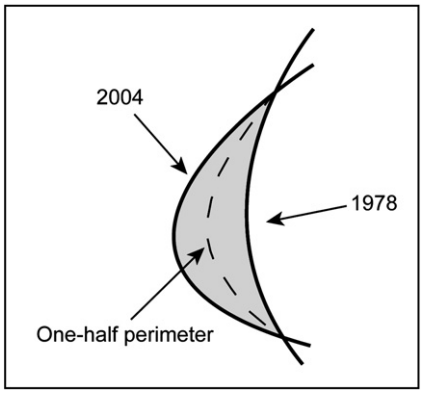

Fig. 2. An eroded-area polygon formed from two channel centerlines. The polygon represents the net centerline shift during the time period from 1978 to 2004. Average polygon migration rate is determined as the polygon area divided by one-half the polygon perimeter and the length of the time period in years (method by Micheli, 2000).

Polygons were classified according to the geology of the bank eroded between 1978 and 2004 using a DWR map of surface geology together with reports of individual Sacramento River bank erosion studies (California Department of Water Resources, 1979, 1994) and field observations. Polygons were classified as terrace material, unconsolidated alluvium with a gravel base (>50% gravel), unconsolidated alluvium with a sandy base, or clay-rich. The most extensive bank material type around a bend was used as the classifier; local variability around single bends was not considered.

Error in the digitized position of channel centerlines was estimated by Micheli et al. (2004) to be an average of about 5% of the total channel width or about 15 m for the Sacramento River. Summing digitization and aerial photograph rectification error in quadrature gives a total error of 21.9 m for a polygon formed from two centerlines. When divided by the time interval of 26 years, the result is an error of ± 0.42 m/y for the average migration rate calculated for a polygon. All polygons with a calculated migration rate less than the error estimate of 0.42 m/y were excluded from the study as were polygons whose growth was restricted by bank-protection structures. This resulted in

the elimination of all but one polygon classified as terrace material. At most sites where the river abuts terrace material, the rate of channel migration is below detection. Of the 27 polygons used in the final analysis, one was classified as terrace, one as clay-rich, one as having a sandy base, and 24 as having a gravel base.

3.2. Calculating bank erosion coefficients using a linear model of meander migration

Bank erosion coefficients for each eroded-area polygon were back-calculated from Eq. (1) following a method by Micheli and Kirchner (2002a) and Micheli et al. (2004). For each polygon with a value of M, the velocity difference u'_b was calculated for the bankfull condition from cross-sectional geometry data and measurements of the planform geometry of the 1978 and 2004 channels.

Ikeda et al. (1981) expressed u'_b as

$$U\frac{\partial u'_b}{\partial s} + 2\frac{U}{H}C_f u' b = b\left[-U^2\frac{\partial c}{\partial s} + C_f c\left(\frac{U^4}{gH^2} + A\frac{U^2}{H}\right)\right] \quad (2)$$

where U is the depth-averaged velocity for the reach, s is streamwise distance, H is the reach-averaged depth, C_f is a friction factor, b is one-half the reach-averaged width, c is local curvature, g is gravitational acceleration, and A is a scour factor defined below. Eq. (2) is derived from the depth-averaged equations for conservation of mass and momentum in a sinuous channel. On the left-hand side of Eq. (2), the first term gives the inertial force resulting from spatial acceleration of flow, and the second term is a portion of the shear force from internal friction. On the right-hand side, the first term accounts for the pressure gradient force resulting from downstream differences in water-surface elevation caused by changes in curvature. The final two terms are components of the shear force from internal friction and account for the effects of super elevation of the water surface and secondary flow, respectively. The friction factor C_f is determined from

$$C_f = \tau / \rho U^2 \quad (3)$$

where ρ is the density of water and τ is defined by

$$\tau = \rho g H S \quad (4)$$

where S is the average longitudinal water-surface slope. After the original formulation by Ikeda et al. (1981), Johannesson and Parker (1988) replaced the scour factor A, a coefficient that characterizes the cross-stream bed slope, with the quantity $A + A_s - 1$. The addition of the term A_s quantifies the effect of the secondary flow in directing the core of high velocity toward the outer bank, and the addition of -1 corrects for an error in earlier work (Johannesson and Parker, 1988). The scour factor A was determined for a cross section using the equation

$$A = -\frac{m}{Hnc} \quad (5)$$

where n is the cross-stream coordinate and m is the local bed elevation (Ikeda et al., 1981). At the channel center, both n and m are 0. The term A_s was calculated for a reach from the formula

$$A_s = 181\left(\frac{H}{b}\right)^2\frac{1}{\chi_1}\left(2\chi^2 + \frac{4}{5}\chi + \frac{1}{15}\right) \quad (6)$$

where

$$\chi_1 = \frac{\alpha}{\sqrt{C_f}},\ \chi = \chi_1 - \frac{1}{3} \quad (7)$$

and α is 0.077 (Johannesson and Parker, 1988). In summary, Eq. (2) accounts for the effects of secondary flow and local and cumulative upstream curvature on the velocity distribution in a bend.

Assuming that u'_b adjusts simultaneously relative to the migration rate M, Eq. (2) may be treated as an ordinary differential equation (Parker and Andrews, 1986) with a solution in the form of

$$u'_b = -\mathrm{bUc} + \frac{\mathrm{bC}_f}{U}\left[\frac{U^4}{\mathrm{gH}^2} + (A+2)\frac{U^2}{H}\right]\cdot\int_0^\infty exp\left(-2C_f s'/H\right)c(s-s')ds' \quad (8)$$

which suggests that u'_b depends primarily on local curvature with upstream curvature exerting a secondary influence (Sun et al., 1996). Sun et al. (1996) found that Eq. (2) could be integrated quickly and accurately by writing $\delta u'_b/\delta s$ as the explicit upstream difference where Δs_i is the streamwise distance between centerline points P_{i-1} and P_i to give

$$u'_{b,i} = \frac{b}{U/\Delta s_i + 2(U/H)C_f}\cdot\left[-U^2\frac{\partial c}{\partial s}|_i + C_f c\left(\frac{U^4}{gH^2} + A\frac{U^2}{H}\right) + \frac{U}{\Delta s_i}\frac{u'b,i-1}{b}\right] \quad (9)$$

Where $\delta c/\delta s$ is calculated as $(c_i - c_{i-1})/\Delta s_i$.

Prior to calculating u'_b for this study, the study area was split into two segments based on differences in channel width and slope (Fig. 1; Table 1). An approximate bankfull discharge Q_b and water-surface slope S were determined for each segment by completing steady flow simulations in HEC-RAS [U.S. Army Corps of Engineers (USACE)] using a set of 380 cross sections extracted from a 1997 seamless channel and floodplain DEM. Bankfull flow was defined as the discharge at which flow began to overtop the point bar or lower bank. For segment 1, this discharge is 2400 m^3/s and corresponds with the 2 year flood at a gauge in the study area (USGS 11389000 at RM 168.5). For segment 2, this discharge is 2000 m^3/s and has a lower recurrence interval of about 1.7 years. Average bankfull width and depth of each segment were determined from the set of cross sections. At each cross section, bankfull elevation was defined as the height of the point bar around bends and the height of the lower bank in straight reaches. Average velocity U was calculated for each segment as $Q_b/2bH$. To check calculated values of U, average velocity was also computed using the Manning equation and with a roughness value (n) of 0.035 (USACE, 2002). The methods resulted in average velocities that differed by 0.1 m/s, or <10%. For each segment, A was determined by linear regression to cross-stream topography data at 10 cross sections chosen at random from among all the cross sections located at bends that were included in the set of 380 cross sections from 1997. Computed values of A are within the expected range for natural streams (Johannesson and Parker, 1988).

In each segment, centerline points were digitized 120 m (0.3 to 0.7 channel widths) apart along the 1978 and 2004 channel centerlines and local curvature was calculated for each point using a procedure by Fagherazzi et al. (2004). At each point, u'_b was determined from Eq. (9), the computed curvature, and the quantities given in Table 1.

Once u'_b was computed for each point along a centerline, the u'_b values were intersected with the eroded-area polygons and the maximum u'_b value in the direction of migration was selected for each polygon (Fig. 3). Because significant changes in the channel centerline and curvature occurred over the 26 years represented by the polygons, an average of the maximum u'_b values selected for the 1978 and 2004

Table 1
Input values for u'_b calculations.

Variable	Segment 1 RM 195-170	Segment 2 RM 170-144
Bankfull discharge Q_b (m^3/s)	2400	2000
Average bankfull width $2b$ (m)	315	210
Average bankfull depth H (m)	4.7	6.3
Average velocity U (m/s)	1.6	1.5
Average slope S	0.00035	0.0002
Friction factor C_f	0.0061	0.0054
Scour factor A	5.9	4.3
Correction A_s	0.2	1.0

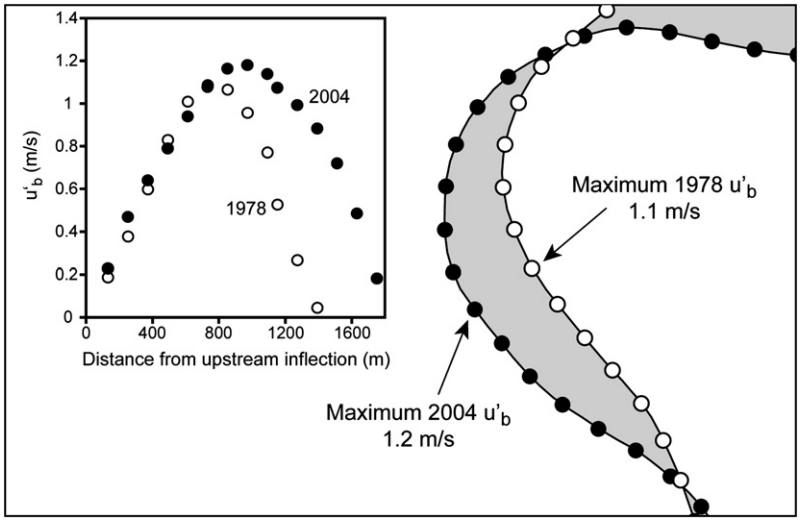

Fig. 3. Example of near-bank velocity difference u_b' calculations around a bend. Arrows show locations of maximum u_b' for the 1978 and 2004 centerlines. The inset shows u_b' at every point between the upstream and downstream inflections of the bend. As a result of channel shifting between 1978 and 2004, the bend is longer in 2004.

centerlines was determined for each polygon. This average is an index of the maximum shear force exerted on the outer bank during the 26 year time period. The average maximum u_b' and migration rate M calculated for the polygon were used to compute E in Eq. (1). As pointed out by Micheli and Kirchner (2002a) and Micheli et al. (2004), E values determined using this method are conservative because they are computed from maximum u_b' values for the polygon.

3.3. Measuring erodibility in the field

To determine the dependence of E on the physical properties of the bank material, the erodibility of different bank types was measured in the field using a jet-test apparatus (Hanson, 1990; ASTM, 1995). The jet-test procedure was developed to obtain estimates of an erodibility coefficient (k) and critical shear stress (τ_c) that are based on direct measurements of bank erosion under known, realistic fluid stress conditions. The calculated k and τ_c can be used to predict erosion by fluvial shear (ε) according to the following relationship:

$$\varepsilon = k(\tau_e - \tau_c) \tag{10}$$

where τ_e is the effective shear stress. The jet as implemented for this study applies a known shear stress to a horizontal streambank surface and the amount of resulting vertical erosion is measured frequently over a period of 1 to 2 h. From the observed relationship between measured erosion depth and time, an equilibrium depth of scour can be determined and τ_c and k calculated. Examples of the change in scour depth with time for two different bank material types are shown in Fig. 4.

Procedures for operating the jet-test apparatus and computing τ_c and k from the collected data are described in detail by Hanson et al. (2002) and Hanson and Cook (2004). Two primary assumptions of the procedures are that the equilibrium depth is the scour depth at which the stress at the boundary is no longer sufficient to cause additional downward erosion (i.e., critical stress τ_c) and that the rate of change in the depth of scour prior to reaching equilibrium depth is a function of the maximum excess stress applied at the boundary and the erodibility coefficient k (Hanson and Cook, 2004).

For use in streams, the apparatus is adjusted so that the shear stress applied to the bank at the onset of testing is approximately equal to the maximum shear stress that the bank would experience under natural flow conditions (Hanson and Cook, 2004).

In this application, the jet-test apparatus was used to obtain measurements of τ_c and k for four different bank types: terrace, unconsolidated alluvium with a gravel base, unconsolidated alluvium with a sandy base, and clay-rich. Results for a total of eight jet tests conducted at seven sites are reported in this paper. The number of test sites was limited by site access and the locations of bank-protection structures. Relatively few sites were accessible for testing because much of the land adjacent to the river is privately owned and the 10 m-tall outer banks around many bends were eroded so steeply that no bench was present where the testing apparatus could be set up and the tests conducted. The jet-test apparatus is too large to be used from a boat.

Testing was carried out during low flow on actively eroding portions of the bank just below the water surface. We assumed that the material being tested was the same as that composing the bank toe. Because the areas tested were located well below the top of the bank, no vegetation was present in the immediate test area and the bank material contained no root or vegetative matter. Prior to beginning the jet test, a horizontal bench at or below the water-surface was prepared by using a shovel to remove the top layer of bank material and any large irregularities. The jet housing was then secured to the bench.

The initial shear stress applied by the jet was set to be equal to one to three times the average bankfull bed shear stress calculated for the channel at that location. Field measurements of flow in bends have found this to be an accurate estimate of the peak shear stress at the toe of the outer bank around bends (Bathurst et al., 1979; Dietrich et al.,

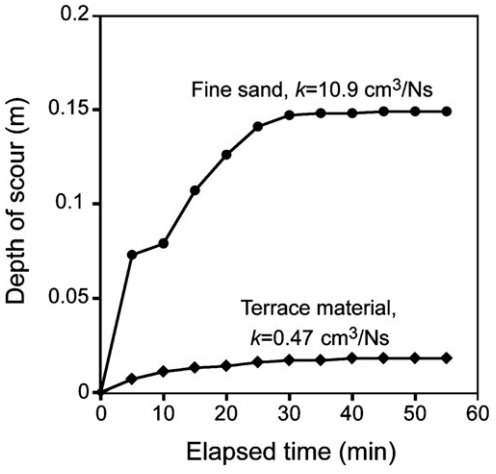

Fig. 4. Examples of the change in scour depth with time observed during the jet-test. Results are shown for two different bank types: fine sand and cemented terrace material.

Table 2
A comparison of migration rate M, u_b', and E for bends with different bank material types.

Bank material classification	Number of polygons	Measured migration rate 1978–2004 (m/y)	Calculated average maximum u_b' (m/s)	Back-calculated E ($x\ 10^{-7}$)
Terrace	1	0.6	0.2	1.0
Clay	1	7.4	1.1	2.1
Sand base	1	10.3	0.6	5.3
Gravel base[a]	24	4.9 ± 2.3 (1.3–9.4)	0.6 ± 0.3 (0.2–1.2)	2.8 ± 1.3 (1.0–5.6)

[a]Average values for banks with a gravel base are ±1 standard deviation; ranges are given in parentheses.

1979). After setting the head tank to deliver the desired initial shear stress, testing was initiated by opening the jet orifice. The vertical depth of erosion was measured every 10 min during the test using a point gauge lowered down through the jet orifice; lowering of the point gauge automatically shuts off the jet for the time it takes to complete the measurement. For cohesive material, testing continued for a total of 1 to 2 h. For noncohesive material, testing was halted when the hole created by the jet began to collapse or became so armored by coarse lag that depth was no longer increasing. The first scenario occurred at sandy banks and the second where banks contain gravel. Our experience has shown that truncating the data in this manner is appropriate and leads to reproducible estimates of τ_c and k.

3.4. Estimating other regression variables

Other variables that have been suggested to influence the magnitude of E in Eq. (1) were estimated or measured for individual bends from aerial photographs, sediment transport modeling, cross-section data, and field data. These variables are floodplain vegetation type (Odgaard, 1987; Pizzuto and Meckelnburg, 1989; Micheli and Kirchner, 2002a; Micheli et al., 2004); proximity to bank-protection structures (Wallick et al., 2006); local average width-to-depth ratio (Larsen, 1995); local average slope (Hasegawa, 1989); local average outer bank height (Hasegawa, 1989); local average velocity (Larsen, 1995); median grain size of the bed at the outer bank (Hasegawa, 1989); and local bed material storage change (Ikeda et al., 1981). Floodplain vegetation type was determined for each eroded-area polygon from 1978 and 2004 aerial photographs. Three major classes were distinguished: forest, agriculture, and unvegetated gravel bar. The vegetative cover type for a polygon was only classified as unvegetated gravel bar for cases where meander migration was primarily in the downstream direction so that relatively young deposits were eroded between 1978 and 2004. Because upstream constraints on migration can influence rates of channel shifting downstream, a measure was chosen to describe the distance between a given polygon and the nearest upstream bank-protection structure. The measure chosen was a count of the number of bends separating the polygon and the protected bend. Average width-to-depth ratio was estimated around each bend where an eroded-area polygon was defined using the set of 1997 cross sections and the definition of bankfull elevation described previously. Average bankfull water-surface slope around each bend was determined for the 2004 channel using the 1997 cross sections and HEC-RAS. Because channel length increased significantly as a result of migration at a number of bends, an estimate of slope for the 1978 channel was also made by adjusting for the difference in centerline length between 1978 and 2004. An average of the slope values for 1978 and 2004 was used to represent the slope around the bend. Outer bank height was taken as the elevation difference between the top of the outer bank and the thalweg. An average value was computed for each bend. From bankfull width, depth, and average slope data, an average downstream velocity was calculated for each bend using the Manning equation. Grain size was not sampled at every eroding bank classified as having gravel at its base; however, extensive bed material sampling was conducted in the main channel in 2004 and 2005 (Singer, in press). Thirty bed material samples taken over the distance from RM 236 to 131, which extends upstream and downstream of the study area, were used to determine a relationship that describes how median grain size declines with distance downstream. The resulting exponential function was used to estimate the median grain size of the bed and lower bank at the location of each eroded-area polygon where the bank was classified as Quaternary alluvium with gravel at its base. Comparison of bed material samples with available bank material samples indicates that the grain size of the bed is a good approximation for the grain size of the lower bank for this bank type. Bed material flux at each of the 380 cross sections was computed using the numerical model FLUVIAL-12 (Chang, 1988a,b). Methods and results for the computations were described in detail by Constantine (2006). The net change in bed material storage around a bend was calculated as the difference between the predicted bed material fluxes at the upstream and downstream cross sections at the bend.

4. Results

4.1. Measured migration rates and calculated values of u_b' and E

For the 27 eroded-area polygons included in the analysis, average migration rates between 1978 and 2004 ranged from 0.6 to 10.3 m/y and calculated values of maximum u_b' ranged from 0.2 to 1.2 m/s (Table 2). Note that the only terrace polygon included was one where lateral migration between 1978 and 2004 was measurable. At other locations where banks are composed of terrace material, lateral shifting was below detection. The greatest value of u_b' determined for a polygon was 1.2 m/s, resulting in a predicted near-bank velocity of 2.8 m/s, or about 1.8 times the average cross-sectional velocity for the segment. This result is within the limits of measured differences between near-bank and cross-sectionally averaged velocities around a bend. In one study, Frothingham and Rhoads (2003) measured maximum depth-averaged velocities, which occurred near the outer bank at curved sections, up to 2.0 and 2.5 times the cross-sectionally averaged velocity.

Bank erosion coefficients (E) calculated from measured migration rates and computed u_b' values ranged from 1.0×10^{-7} to 5.6×10^{-7} (Table 2). Values of E calculated for gravel banks spanned the entire range from 1.0×10^{-7} to 5.6×10^{-7} with 63% of the 24 sites having a value between 1.0×10^{-7} and 3.0×10^{-7} (Fig. 5). Values of E shown in Table 2 are similar to those calculated previously for the Sacramento

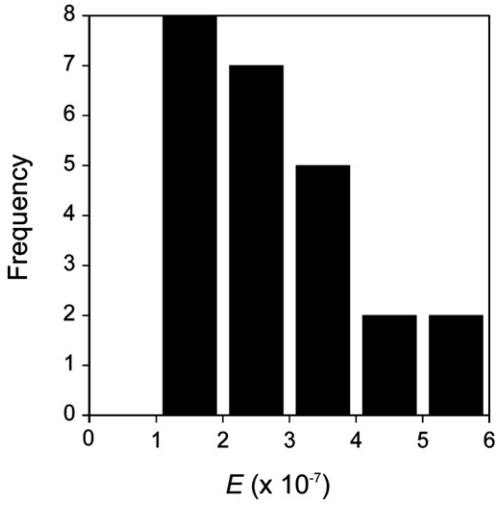

Fig. 5. Frequency distribution of E values calculated from historical data of planform change over 26 years for the 24 eroding banks in the study area classified as having a basal gravel layer.

Table 3
Bank erodibility and critical shear stress from field measurements.

Bank type	Number of tests conducted	River mile location(s)	Average k (cm^3/Ns)[a]	Average τ_c (Pa)[a]
Terrace	1	164.5	0.5	3.9
Clay-rich	2	197, 182.7	2.2 (1.3, 3.1)	0.02 (0.01, 0.03)
Sand base	2	193.1	11.6 (10.9, 12.2)	0.07 (0.01, 0.1)
Gravel base	2	193.2, 171.5	1.2 (1.1, 1.4)	2.2 (1.6, 2.8)

[a]Data for individual tests are given in parentheses.

River by Micheli et al. (2004). Micheli et al. (2004) did not segregate their results by bank type.

When considering the average values computed for each bank type, the erosion coefficient appears to depend strongly on bank composition, with banks composed of terrace material having the lowest coefficients and banks composed of unconsolidated sand having the highest coefficients (Table 2).

4.2. Jet-test results

Erodibility coefficients (k), which quantify bank resistance to erosion by fluvial shear, and estimates of critical shear stress (τ_c) computed from field data are given in Table 3. As described in the methods section, k is a function of the measured rate of erosion and τ_c is a function of the equilibrium scour depth. According to the computed k values, banks composed of terrace material exhibit the greatest resistance to erosion followed by noncohesive banks that contain gravel, banks composed of clay-rich material, and banks composed of sand. With regard to noncohesive banks, those that are composed primarily of sand are about 10 times more erodible than those that include a gravel basal layer.

The data for the terrace bank type was collected at a location where the jet housing apparatus could be hammered into the bank. Erosion of the material during the test occurred through slaking of aggregates rather than through particle-by-particle erosion. The testing site is the one mentioned in the previous section as undergoing measurable lateral migration between 1978 and 2004. At other terrace sites, the banks were cemented to such an extent that the jet housing could not be set into the bank material and no test could be performed. For these cases, k should be essentially zero.

To quantify the grain size of the clay-rich banks, two samples, one from each of the test sites, were sieved in the lab and found to contain 83 and 90% silt and clay with 17 and 7% sand. Much of the sand occurred in fine lenses that eroded relatively easily during the jet testing, and the site with the higher sand content exhibited higher erodibility.

For cohesive streambeds in the midwestern United States, Hanson and Simon (2001) found a nonlinear inverse relationship between k and τ_c:

$$k = 0.2\tau_c^{-0.5} \tag{11}$$

The data collected for this study plot on the curve (Hanson and Simon, 2001; Fig. 8) in the areas the authors labeled as “very erodible” and “erodible.”

Critical shear stress (τ_c) computed from the jet-test results was lowest for the clay-rich banks and highest for banks composed of cemented terrace material and those composed of gravel. The critical shear stress as defined here is the shear stress at which vertical erosion of the hole formed by the jet ceases (Hanson and Cook, 2004). This is different from the shear stress required to initiate motion of particles from a planar bed surface. In the case of the jet-test procedure, the flow must exert sufficient force on a particle to initiate motion and carry it out of the vertical scour hole, which can be 10 or more centimeters in depth (i.e., many times greater than the particle diameter). This discrepancy in the definition of τ_c explains why values obtained from the jet-test results are lower for clay- and silt-sized material than for sand-sized material, a result that contradicts published literature on the topic (see Vanoni, 2006). Upon approaching the equilibrium scour depth at sandy banks, grains were still in motion at the bottom of the scour hole but were unable to be excavated from the hole. For this reason, we believe that k, which is a function of the observed rate of bank material erosion during the jet test, is a better measure of bank material resistance to fluvial shear than computed τ_c, which particularly in the case of noncohesive bank material is overestimated as a function of the measured equilibrium depth of scour rather than the onset of particle motion.

4.3. Correlation between E and erodibility determined from field data

Values of E were calculated for a total of 27 bends: one with banks classified as terrace, one with clay-rich banks, one with banks that have a sandy base, and 24 with banks with a gravel base. Although jet tests were performed at a total of seven sites, only three of those sites were located at freely migrating bends for which E was calculated because of the difficulty in accessing actively eroding banks. The other four sites where jet tests were performed were located at bends where migration was partially constrained; therefore, E values were not calculated. The three sites with coincident E and k data included locations with bank material classified as terrace, clay-rich, and gravel (square symbols in Fig. 6). For sandy bank material, the calculated E value was paired with k determined from a jet test performed on a different sandy bank (circle symbol in Fig. 6).

The result of a linear regression between E calculated from Eqs. (1) and (2) and k determined from field data is shown in Fig. 6. Although the sample size of Fig. 6 is small because of the difficulty in accessing eroding banks for jet-testing, the relationship shown suggests that the variability in the calculated bank erosion coefficient E is dominated by differences in bank material composition and associated resistance to fluvial shear. The correlation is consistent with the understanding that u_b', which was used to calculate E, reflects the magnitude of the shear force exerted on the bank and the grain-scale resistance to shearing. One implication of a correlation between E and k is that vegetation plays a limited role in determining long-term migration rates in the Sacramento River. This suggestion will be discussed more fully in the next section.

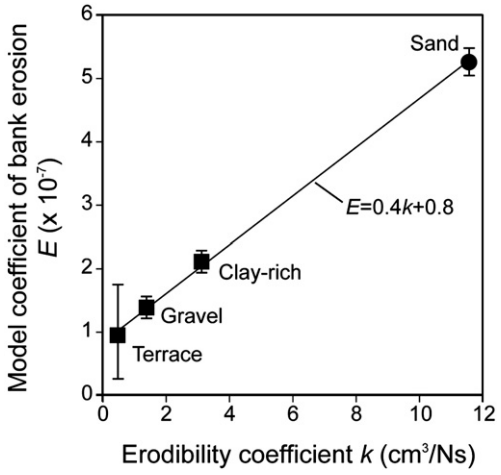

Fig. 6. Coefficient of bank erosion E calculated from historical data of planform change over 26 years using Eqs. (1) and (9) plotted against erodibility coefficient k determined from field measurements. Values of k represent bank material properties alone. Each data point represents a different bank type: terrace, clay-rich, gravel, or sand. The square data points show coincident E and k values for a given bend (i.e., the jet-test was performed at the same bank for which E was calculated). Coincident E and k values were available for only one of the 24 bends with gravel banks in the study area because of the difficulty in accessing actively eroding banks for jet-testing. For the data point shown as a circle, the calculated E value was paired with a k value determined from a jet-test performed on a sandy bank at a different location. Error bars show the uncertainty associated with measurement of the historical migration rates used to calculate E.

4.4. Variability of E values for gravel banks

As described above, values of E calculated for the 24 banks with gravel basal layers ranged from 1.0×10^{-7} to 5.6×10^{-7} with 63% of the sites having a value between 1.0×10^{-7} and 3.0×10^{-7} (Fig. 5; Table 2). Jet-test results suggest that this variability is a result of differences in bank material properties despite a common broad classification. At RM 193.2, for example, the basal gravel layer has a D_{50} of 10.6 mm and contains 25% sand. The computed erodibility k at this location was 1.1 cm^3/Ns (Table 3). At RM 171.5, the basal gravel layer has a smaller D_{50} of 5.4 mm and has a higher sand content of 40%. The gravel layer at this location had a higher computed erodibility k of 1.4 cm^3/Ns (Table 3). This difference in bank material properties and erodibility represents the type of variability captured by E values computed from measured historical migration rates.

In the absence of jet-test data for all 24 gravel sites, E values were correlated with the median grain size of the bed at the outer bank, interpolated from bed material sampled by Singer (in press) that fines gradually downstream. A statistically significant but weak negative correlation was found between E and D_{50} at the outer bank around a bend ($r^2=0.2$, $\alpha=0.05$). Analysis of the bed material samples showed that sand content increases linearly with the decreasing logarithm of D_{50} ($r^2=0.95$). The negative correlation with D_{50} therefore implies that as noncohesive bank material grain size declines and/or sand content increases, the migration rate for a given u_b' increases. This suggests that better quantification of erodibility of different gravel banks using the jet test would produce additional pairs of E and k that would plot on the curve shown in Fig. 6.

Other macroscale, site-specific variables were examined to determine if any factors other than grain-scale differences in bank material resistance to fluvial shear contributed to the wide variability observed in E values calculated for gravel banks. Four nominal-scale factors were examined: floodplain land cover (forest, agriculture, or unvegetated gravel bar), proximity to upstream bank-protection structures (distance less than or equal to or greater than one bend length), average segment velocity U (1.4 or 1.6 m/s), and bed material storage change around the bend (net bed material erosion or deposition). Two-tailed t-tests were performed at a 5% level of significance for each factor to evaluate whether the classification distinguishes between the means of different samples of E values.

We found that mean E values corresponding to the three different land cover classifications cannot be considered significantly different. For the other three factors, proximity to bank protection, average segment velocity, and bed material storage change, the null hypothesis of equal sample means was rejected, indicating that local differences in these variables are incorporated into E. The mean values of E corresponding to each classification are given in Table 4. Calculated E values are greater around bends where net bed material storage change is positive (net deposition) than around bends where net bed material storage change is negative (net erosion). This suggests that low availability of bed material for deposition on bars may have a limiting effect on long-term meander migration rates in the Sacramento River. In the linear model represented by Eq. (1), this effect is not described in the expression for u_b' and is therefore incorporated into the calibrated coefficient of bank erosion E. Thus if back-calculated values of E are used as measures of bank erodibility, banks will appear more erodible around bends experiencing net bed material deposition. This result is not a contradiction of Eq. (1) but may simply indicate that cross-sectional changes in an aggrading or degrading stream affect the flow field and would ideally be taken into account by constantly updated channel surveys. Otherwise, unaccounted changes in the cross-channel advection of flow will be incorporated into the coefficient E.

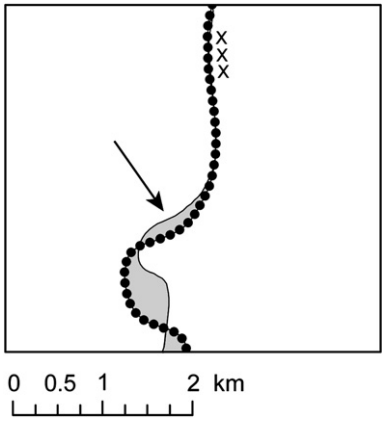

Fig. 7. An example of a bend where the back-calculated E value is low and its position relative to upstream bank-protection. The arrow indicates the eroded-area polygon (hatched) for which E is low. The upstream bank-protection structure is shown by the crosses. The dots are the points along the 2004 channel centerline for which u_b' was calculated. Calculations of u_b' were also made along the 1978 channel centerline (points not shown here).

The data in Table 4 show that E values are lower at bends located immediately downstream of bank-protection structures. In general, protected reaches preceding the bends in question are relatively long and straight, exhibiting curvature that is low but constant in sign (Fig. 7). Because computed u_b' depends on the sign or direction of curvature and is cumulative [see the last term in Eq. (9)], u_b' increases through the protected reach and into the downstream bend where it reaches a maximum just before the inflection. Migration of the bend is relatively low despite high u_b' because the upstream limb of the bend (i.e., the protected reach) is pinned and unable to translate downstream. This combination of low migration rate M but high u_b' results in a low value of E as calculated using Eq. (1).

At first consideration, the result of greater E values in the downstream segment where cross-sectionally averaged velocity U is lower (Table 4) is puzzling because segment velocity is already accounted for in the U term in the expression for u_b' [Eq. (9)]. This suggests that the difference in E is actually reflecting a downstream change in some other parameter. The most probable explanation is that the difference in E is related to the downstream reduction in grain size and increase in sand content discussed above.

In addition to the four nominal-scale factors listed above, four measurements of flow and channel characteristics around bends were examined for correlations with E: local width-to-depth ratio, local slope, local bank height, and local cross-sectionally averaged velocity. Because the direction of local bed material storage change was found above to be a significant factor in determining E, the magnitude of storage change was included as a fifth variable. No significant correlation was found between E and local width-to-depth ratio, slope, bank height, or velocity. This suggests that the average conditions (b, S, H, U) used in the formula for u_b' [Eq. (9)] sufficiently represent the channel and flow characteristics in each segment. Correlations with E would be expected if substantial local variability not captured by Eq. (9) was producing measurable differences in rates of meander migration. A statistically significant but weak positive correlation was found between E and bed material storage around a bend ($r^2=0.2$, $\alpha=0.05$). This correlation was anticipated based on the result of the t-test above.

Table 4
Results of t-tests performed on E values for gravel banks.

Factor	Mean E[a] (x 10^{-7})		p-value from t-test
	Positive change	Negative change	
Bed material storage change around bend	3.5 ± 14 1.4 m/s	2.1 ± 0.7 1.6 m/s	0.005
Average segment velocity U	3.6 ± 1.3 1 bend	2.2 ± 0.9 >1 bend	0.01
Distance to nearest upstream bank-protection structure	2.1 ± 0.8	3.1 ± 1.3	0.02

[a]Mean E values are ±1 standard deviation.

5. Discussion of results

5.1. Sources of error in the correlation between E and k

A potential source of error that may affect the relationship shown in Fig. 6 is the uncertainty in erodibility coefficients (k) obtained from the jet tests. A weakness of the data set collected for this study is that repeated jet tests were not conducted at most sites primarily because of time limits on site access. A certain amount of variability in k measured for a given bank should be expected as a result of local variability in bank material grain size and, in the case of cohesive bank material, subaerial exposure and weathering (Hanson and Simon, 2001). During testing for this study, variability resulting from varying degrees of subaerial exposure and weathering were minimized by first scraping away the surface of the bank before attaching the jet housing. At one bank composed of sandy material, two jet tests produced k values of 10.9 and 12.2 cm^3/Ns, which differ by ~10% (Table 3). The 10.9 cm^3/Ns value corresponds to a location on the bank with finer sand and 12.2 cm^3/Ns corresponds to a location on the bank with coarser sand, as identified by field inspection. Repeated testing of cohesive banks by Hanson and Simon (2001) yielded differences in k values of 0 to over 100% attributed to grain size variation at a single site.

Another question that may be raised is whether E and k are functions of the same component of the total shear stress acting on a river bank. In a river bend, the total boundary shear stress acting on the outer bank is the sum of stress resulting from drag on bedforms and the stress acting on the actual boundary. Smith and McLean (1977) and, more recently, Kean and Smith (2006) gave methods for partitioning the total shear stress into form drag and skin friction, or the stress acting on the boundary. In the jet-test procedure used to calculate k, a stress was applied directly to the smoothed, unvegetated bank surface in a focused manner, precluding quantification of the influence of bank roughness elements. With regard to E, the migration rate [M in Eq. (1)] used in its calculation is a record of the rate of sediment removal from the base of the bank and is therefore a function of skin friction. The migration rate M is then correlated with u'_b, which represents the total shear stress and does not take bank effects into account; therefore, the influence of bank roughness would be incorporated into E. The correlation of E with k (Fig. 6), however, suggests that E values for the Sacramento River reflect the dominance of skin friction, or the grain-scale resistance to fluid shear. This finding is specific to eroding banks like those of the Sacramento River that are tall and generally free of low hanging vegetation and resistant failed blocks.

5.2. The relationship between E and k

A relationship between E and k as suggested by Fig. 6 is consistent with the current understanding that the rate of bank erosion ultimately depends on the rate of removal of material from the base of the bank by fluvial entrainment (Thorne, 1982). This is true where the primary mechanism of bank retreat is mass failure or fluvial shear. In the Sacramento River, most actively eroding banks are unconsolidated alluvium with a lower layer of noncohesive gravel and sand and an upper layer of silt that fails via cantilever failure (K. Buer, DWR, personal communication, 2002). Based on field inspection, the failed blocks of silt are typically easily eroded once wet; therefore, the rate of bank retreat is controlled by the rate at which the coarser material at the base of the bank is eroded.

An encouraging implication of the correlation in Fig. 6 is the possibility that the bank erosion coefficient E may be determined directly from field measurements of bank material resistance to fluvial shear, allowing for predictions of meander migration that are independent of past patterns of channel shifting. This interpretation is subject to further testing under a wider range of conditions to augment the data presented here.

Also subject to further testing is the hypothesis that the relationship between E and k shown in Fig. 6 varies with the size of the river. Larsen (1995) found that E values are substantially higher for the Mississippi River than for small creeks and concluded that E includes a scale effect, which remains to be identified and explained but may depend on the effect of bank height on slope stability, tree reinforcement of low banks, or scale-related flow-duration regimes that extend the duration of competent flows in large rivers. The data presented here derive from only a single large lowland river.

5.3. The role of vegetation

An important implication of the correlation between E and k is that riparian vegetation, the effects of which were not measured by the jet-test device, plays a limited role in determining long-term bank erosion rates in the Sacramento River. This hypothesis is supported by a small number of other studies, while most of the existing literature on the topic concludes that the influence of vegetation on bank erosion is significant. This apparent contradiction warrants further discussion.

Numerous researchers have found elsewhere that vegetation can act to stabilize banks against failure (Abernethy and Rutherfurd, 2000; Micheli and Kirchner, 2002b; Simon and Collison, 2002) and retard near-bank flow velocity (Pizzuto and Meckelnburg, 1989; Thorne and Furbish, 1995). On the other hand, recent work utilizing a new model of bank stability has shown that the influence of mature, woody vegetation on bank stability, excluding any vegetation effects on pore water pressures, is small relative to the influence of other bank properties such as bank height and bank material composition (Van De Wiel and Darby, 2007). In terms of erosion of failed or intact bank material by fluvial shear, vegetation that protrudes into the flow may actually enhance local turbulence and bank scour (Lawler et al., 1997), and fallen trees may redirect flow toward the eroding bank.

In considering the results of this and other studies, the problem of whether or not the presence of vegetation affects migration rates appears to be a question of scale and time frame. In rivers and streams where bank height is less than rooting depth, vegetation can be expected to increase the shear strength of the bank (e.g., Micheli and Kirchner, 2002b; Van De Wiel and Darby, 2007) and bind together noncohesive bank material. Wynn and Mostaghimi (2006) applied the submerged jet test to vegetated banks along small streams with bank exposures above base flow ranging from 65 to 225 cm and drainage areas between 9 and 322 km^2. The authors found that in this type of setting root density has a significant impact on bank material erodibility under fluid shear.

Average bank height in the Sacramento River is 8 to 10 m, greater than the 2 to 4 m maximum rooting depths of woody riparian species of the Sacramento Valley such as valley oak (*Quercus lobata*), California black walnut (*Juglans californica*), and Oregon ash (*Fraxinus latifolia*) (Canadell et al., 1996; Alpert et al., 1999), and the much shallower layer of dense roots. The large size of the Sacramento River channel, therefore, brings into question the impact of vegetation on geotechnical bank stability and also on rates of erosion via fluvial shear. Where vegetation is confined to the tops of tall cutbanks, it can resist tension cracking and exert a minor influence on the shear strength across a potential failure surface, but not on the rate of the erosion at the toe of the bank, which eventually undermines even root-reinforced slopes. In this study, no vegetative matter (including root material) was observed low on the banks where the jet tests were conducted. Furthermore, the average angle of eroding banks along the Sacramento River is 30 to 35° from the top of the bank to the bank toe, equivalent to the angle of repose of unconsolidated gravel and sand. Fig. 6 suggests that for the Sacramento and perhaps other large rivers any vegetation effects on bank erosion rates are small compared with the influence of bank material composition on resistance to fluvial shear. Nanson and Hickin (1986) discussed a similar implication of their data for 18 large rivers in Canada with widths ranging from 30 to 278 m and bank heights

ranging from 2 to 8.3 m; vegetation on tall banks does little to increase geotechnical stability or protect the subaqueous portion of the bank from boundary shear.

Micheli et al. (2004) calculated bank erosion coefficients (E) from Sacramento River planform data for three different time periods (1946–1969, 1981–1991, and 1991–1997) and compared values for bends adjacent to forested and agricultural land. The authors found that E values calculated for forested reaches were consistently lower than those calculated for agricultural reaches. Equating E to bank erodibility, the authors argued that forested floodplain is less erodible than agricultural floodplain, reflecting primarily the slowing of near-bank velocities by bank vegetation and debris along forested banks. As mentioned briefly by the authors, the data showed a greater difference between E values for forested and agricultural floodplain sections over the two shorter time periods than over the longer time period.

Both forested and unforested banks along the Sacramento River experience erosion at the bank toe that causes undercutting and eventually collapse. Qualitative field observations made for this study suggest that large failed, root-bound blocks of sandy–silty soil from the forested floodplain temporarily form a buffer to flow that persists through at least the low-flow season following failure. It is unknown whether the blocks, which are a few meters wide, persist through one or more high-flow seasons. The failures observed at forested banks during the course of this study were ~10 times wider than those observed at unvegetated or sparsely vegetated banks. The large size of the failures, therefore, may compensate over the long term for the retarding effects of failed blocks on bank erosion rates over the short term. This may explain why Micheli et al. (2004) documented larger differences in E between forested and agricultural banks for 6 and 10 year time periods than for a 20 year time period. As described in an earlier section, no statistically significant difference was detected between mean E values at gravel banks corresponding to three different land cover classifications (forest, agriculture, and unvegetated gravel bar) for the 26 year time period examined in this study.

6. Conclusions

The jet-test apparatus provides a quantitative measure of bank material resistance to fluvial shear (k) for both cohesive and noncohesive banks. For a small data set that includes both types of banks along the Sacramento River, a linear relationship was found between the bank erosion coefficient E, back-calculated from data on long-term meander migration rates and channel characteristics, and k measured using the jet test. Erodibility k computed in this study depends only on bank material composition and does not incorporate effects of vegetation, yet differences in k largely explain the variability observed in E values at different banks, at least for the limited data set presented here. One implication of this result is that vegetation may play an insignificant role in determining long-term meander migration rates of the Sacramento River and other large rivers. Although a number of previous studies support this hypothesis, work is needed to clarify the role of vegetation while controlling for the size of the river and the timescale of migration rate measurement.

The strong correlation between E and k suggests that E is primarily a function of bank material properties; however, further examination of results for banks with gravel bases indicate that other variables may play minor roles in determining E. Values of E are significantly lower immediately downstream of bank-protection structures than elsewhere. Upstream bank protection affects the planform geometry and stability and therefore the flow field at the entrance to the top of a reach where bank erosion is measured; disproportionately high values of u_b' but low values of M in the reach yield low values of E. In addition, a weak positive correlation was found between E and net bed material storage change, indicating the importance of accounting for availability of bed material for deposition when making predictions of meander migration rates. It remains to be resolved whether this effect can be accounted for by frequently updating the channel geometry inputs to Eq. (9) from field surveys or modeling of bed material storage changes.

Both the jet test over a wide range of bank material grain sizes and the statistical analyses of factors affecting the bank erosion coefficient E at gravel banks indicate the importance of texture-scale geotechnical controls in determining bank resistance to erosion, and therefore meander migration rates, once flow and channel curvature have been accounted for. Results from the Sacramento River suggest the possibility that modeling long-term meander migration of large rivers may be facilitated by estimating the coefficient of bank erosion E directly from field measurements of bank material resistance to erosion by fluvial shear. Given the opportunity for enhancing predictive capabilities and addressing river engineering problems, this implication warrants additional testing on other large rivers with a range of bank material types.

Acknowledgements

We thank José Constantine and Julien Levrat for assistance in the field and the U.S. Fish and Wildlife Service, especially Kelly Maroney and Joe Silvera, for granting access to sites on the Sacramento River Wildlife Refuge. This paper was greatly improved by reviews from Stephen Darby and James Pizzuto. Support for this research was provided by CALFED grant 4600002659, the Geological Society of America Easterbrook award, and the Department of Earth Science at the University of California, Santa Barbara.

References

Abernethy, B., Rutherfurd, I.D., 2000. The effect of riparian tree roots on the mass-stability of riverbanks. Earth Surf. Process. Landf. 25, 921–937.
Alpert, P., Griggs, F.T., Peterson, D.R., 1999. Riparian forest restoration along large rivers: initial results from the Sacramento River project. Restor. Ecol. 7, 360–368.
American Society For Testing And Materials (ASTM), 1995. Annual Book of ASTM Standards: Section 4. Construction. ASTM, West Conshohocken, PA.
Bathurst, J.C., Thorne, C.R., Hey, R.D., 1979. Secondary flow and shear stress at river bends. J. Hydraul. Eng. Div.—ASCE 105, 1277–1295.
Brunsden, D., Kesel, R.H., 1973. Slope development on a Mississippi River bluff in historic time. J. Geol. 81, 576–598.
California Department of Water Resources, 1979. Observations of Sacramento River Bank Erosion 1977–1979. Calif. Dept. Water Resour., Northern District, Red Bluff, CA.
California Department of Water Resources, 1994. Sacramento River Bank Erosion Investigation Memorandum Progress Report. Calif. Dept. Water Resour., Northern District, Red Bluff, CA.
Canadell, J., Jackson, R.B., Ehleringer, J.R., Mooney, H.A., Sala, O.E., Schulze, E.-D., 1996. Maximum rooting depth of vegetation types at the global scale. Oecologia 108, 583–595.
Chang, H.H., 1988a. Introduction to FLUVIAL-12: mathematical model for erodible channels. In: Fan, S. (Ed.), Twelve Selected Computer Stream Sedimentation Models Developed in the United States. Federal Energy Regulatory Commission, Washington, D.C., pp. 353–412.
Chang, H.H., 1988b. Fluvial Processes in River Engineering. John Wiley & Sons, Inc., New York. 432 pp.
Constantine, C.R., 2006. Quantifying the connections between flow, bar deposition, and meander migration in large gravel-bed rivers. Ph.D. Thesis, Univ. of Calif., Santa Barbara, 191 pp.
Darby, S.E., Alabyan, A.M., Van de Wiel, M.J., 2002. Numerical simulation of bank erosion and channel migration in meandering rivers. Water Resour. Res. 38, 1163. doi:10.1029/2001WR000602.
Dietrich, W.E., Smith, J.D., Dunne, T., 1979. Flow and sediment transport in a sand bedded meander. J. Geol. 87, 305–315.
Fagherazzi, S., Gabet, E.J., Furbish, D.J., 2004. The effect of bidirectional flow on tidal channel planforms. Earth Surf. Process. Landf. 29, 295–309.
Frothingham, K.M., Rhoads, B.L., 2003. Three-dimensional flow structure and channel change in an asymmetrical compound meander loop, Embarras River, Illinois. Earth Surf. Process. Landf. 28, 625–644.
Hanson, G.J., 1990. Surface erodibility of earthen channels at high stresses. Part II—developing an in situ testing device. T. Am. Soc. Agric. Eng. 33, 132–137.
Hanson, G.J., Cook, K.R., 2004. Apparatus, test procedures, and analytical methods to measure soil erodibility in situ. Appl. Eng. Agric. 20, 455–462.
Hanson, G.J., Simon, A., 2001. Erodibility of cohesive streambeds in the loess area of the midwestern USA. Hydrol. Process. 15, 23–38.
Hanson, G.J., Simon, A., Cook, K.R., 2002. Non-vertical jet testing of cohesive streambank materials. ASAE Meeting Paper, vol. 022119. ASAE, St. Joseph, MI.
Hasegawa, K., 1989. Universal bank erosion coefficient for meandering rivers. J. Hydraul. Eng. 115, 744–765.

Howard, A.D., 1992. Modelling channel migration and floodplain development in meandering streams. In: Carling, P.A., Petts, G.E. (Eds.), Lowland Floodplain Rivers. John Wiley & Sons, Chichester, UK, pp. 1–42.
Ikeda, S., Parker, G., Sawai, K., 1981. Bend theory of river meanders. Part 1. Linear development. J. Fluid Mech. 112, 363–377.
Johannesson, H., Parker, G., 1988. Inertial effects on secondary and primary flow in curved channels. External Memorandum No. 208. St. Anthony Falls Hydr. Lab., Univ. of Minn.
Johannesson, H., Parker, G., 1989. Linear theory of river meanders. In: Ikeda, S., Parker, G. (Eds.), River Meandering. American Geophysical Union, Washington, D.C., pp. 181–213.
Kean, J.W., Smith, J.D., 2006. Form drag in rivers due to small-scale natural topographic features: 1. Regular sequences. J. Geophys. Res. 111, F04009.
Larsen, E.W., 1995. Mechanics and modeling of river meander migration. Ph.D. Thesis, Univ. of Calif., Berkeley.
Larsen, E.W., Greco, S.E., 2002. Modeling channel management impacts on river migration: a case study of Woodson Bridge State Recreation Area, Sacramento River, California, USA. Environ. Manage. 30, 209–224.
Larsen, E.W., Girvetz, E.H., Fremier, A.K., 2006. Assessing the effects of alternative setback channel constraint scenarios employing a river meander migration model. Environ. Manage. 37, 880–897.
Lawler, D.M., Thorne, C.R., Hooke, J.M., 1997. Bank erosion and instability. In: Thorne, C. R., Hey, R.D., Newson, M.D. (Eds.), Applied Fluvial Geomorphology for River Engineering and Management. John Wiley & Sons, Chichester, UK, pp. 137–172.
Micheli, E.R., 2000. Quantifying the effects of riparian vegetation on river meander migration. Ph.D. Thesis, Univ. of Calif., Berkeley.
Micheli, E.R., Kirchner, J.W., 2002a. Effects of wet meadow riparian vegetation on streambank erosion. 1. Remote sensing measurements of streambank migration and erodibility. Earth Surf. Process. Landf. 27, 627–639.
Micheli, E.R., Kirchner, J.W., 2002b. Effects of wet meadow riparian vegetation on streambank erosion. 2. Measurements of vegetated bank strength and consequences for failure mechanics. Earth Surf. Process. Landf. 27, 687–697.
Micheli, E.R., Kirchner, J.W., Larsen, E.W., 2004. Quantifying the effects of riparian forest versus agricultural vegetation on river meander migration rates, central Sacramento River, California, USA. River Res. Appl. 20, 537–548.
Nagata, N., Hosoda, T., Muramoto, Y., 2000. Numerical analysis of river channel processes with bank erosion. J. Hydraul. Eng. 126, 243–252.
Nanson, G.C., Hickin, E.J., 1986. A statistical analysis of bank erosion and channel migration in western Canada. Geol. Soc. Amer. Bull. 97, 497–504.
Odgaard, A.J., 1987. Streambank erosion along two rivers in Iowa. Water Resour. Res. 23, 1225–1236.
Parker, G., Andrews, E.D., 1986. On the time development of meander bends. J. Fluid Mech. 162, 139–156.
Pizzuto, J.E., Meckelnburg, T.S., 1989. Evaluation of a linear bank erosion equation. Water Resour. Res. 25, 1005–1013.
Simon, A., Collison, A.J.C., 2002. Quantifying the mechanical and hydrologic effects of riparian vegetation on streambank stability. Earth Surf. Process. Landf. 27, 527–546.
Singer, M.B., in press. Downstream patterns of bed-material grain size in a large, lowland alluvial river subject to low sediment supply. Water Resour. Res. doi:10.1029/2008WR007183.
Singer, M.B., 2007. The influence of major dams on hydrology through the drainage network of the Sacramento River basin, California. River Res. Appl. 23, 55–72.
Smith, D.W., Verrill, W.L., 1998. Vernal pool-soil-landform relationships in the Central Valley, California. In: Witham, C.W., Bauder, E.T., Belk, D., FerrenJr. Jr., W.R., Ornduff, R. (Eds.), Proceedings, Ecology, Conservation, and Management of Vernal Pool Ecosystems, 1996. Calif. Native Plant Soc., Sacramento, CA, pp. 15–23.
Smith, J.D., McLean, S.R., 1977. Spatially averaged flow over a wavy surface. J. Geophys. Res. 82, 1735–1746.
Stølum, H.H., 1998. Planform geometry and dynamics of meandering rivers. Geol. Soc. Amer. Bull. 110, 1485–1498.
Sun, T., Meakin, P., Jøssang, T., 1996. A simulation model for meandering rivers. Water Resour. Res. 32, 2937–2954.
Sun, T., Meakin, P., Jøssang, T., 2001a. Meander migration and the lateral tilting of floodplains. Water Resour. Res. 37, 1485–1502.
Sun, T., Meakin, P., Jøssang, T., 2001b. A computer model for meandering rivers with multiple bed load sediment sizes. 2. Computer simulations. Water Resour. Res. 37, 2243–2258.
Thorne, C.R., 1982. Processes and mechanisms of river bank erosion. In: Hey, R.D., Bathurst, J.C., Thorne, C.R. (Eds.), Gravel-bed Rivers: Fluvial Processes, Engineering, and Management. John Wiley & Sons, New York, pp. 227–271.
Thorne, C.R., Tovey, N.K., 1981. Stability of composite river banks. Earth Surf. Process. Landf. 6, 469–484.
Thorne, S.D., Furbish, D.J., 1995. Influences of coarse bank roughness on flow within a sharply curved river bend. Geomorphology 12, 241–257.
United States Army Corps of Engineers (USACE), 2002. Technical Studies Documentation. Appendix A: Information Papers. Sacramento and San Joaquin River Basins Comprehensive Study. USACE, Sacramento, CA.
Van De Wiel, M.J., Darby, S.E., 2007. A new model to analyse the impact of woody riparian vegetation on the geotechnical stability of riverbanks. Earth Surf. Process. Landf. 32, 2185–2198.
Vanoni, V.A., 2006. Sedimentation Engineering: Manuals and Reports on Engineering Practice No. 54. ASCE Publications, Reston, VA. 418 pp.
Wallick, J.R., Lancaster, S.T., Bolte, J.P., 2006. Determination of bank erodibility for natural and anthropogenic bank materials using a model of lateral migration and observed erosion along the Willamette River, Oregon, USA. River Res. Appl. 22, 631–649.
Wynn, T., Mostaghimi, S., 2006. The effects of vegetation and soil type on streambank erosion, southwestern Virginia, USA. J. Am. Water Resour. Assoc. 42, 69–82.